Research Article

Journal of Chemistry Letters
journal homepage: www.jchemlett.com
ISSN (online) 2717-1892 (print) 2821-0123

Systematic investigation of inter-element effects during EDXRF measurements on mixed oxide powders of aluminium, silicon, and yttrium

P.S. Remya Devi[1,*], T.A. Chavan[1], M. Sarma and K.K. Swain[1]

[1]*Analytical Chemistry Division, Bhabha Atomic Research Centre, Trombay, Mumbai, India*

ARTICLE INFO

Article history:
Received 12 July 2023
Received in revised form 27 October 2023
Accepted 27 October 2023
Available online 27 October 2023

Keywords:
inter-element effects
EDXRF
yttrium aluminium silicate
powder samples

ABSTRACT

Inter-element effects may severely affect the accuracy during EDXRF measurements of mixed oxides. Single (individual), binary and ternary oxide mixtures of Al, Si and Y were made with cellulose and the pellets were prepared. Sensitivity and intercept of the EDXRF spectrometer for Al, Si and Y were determined. Effects of presence of the other elements on the sensitivity and intercept were studied. The sensitivity was found to increase, as per the atomic number. Characteristic X-ray energies, absorption edges and attenuation coefficients are the key factors, which controlled the sensitivity. Presence of interfering impurities, overlap of peaks and X-ray absorption, hold the principal control over intercept of the calibration curves. For each of the three present analytes, the major contributor to inter-element effect was identified, via a systematic approach. Compositions of two samples of yttrium aluminium silicate were determined, after incorporating inter-element correction factors.

1. Introduction

Mixed oxides of yttrium (Y), aluminium (Al) and silicon (Si) are used in the medical field for various diagnostic and therapeutic applications [1, 2]. These are popularly known as "thera-spheres" [3] or "Bhabha-spheres". Quantification of the major constituents, Y, Al, Si, is inevitable for optimizing the amounts and efficacy of the material. Compositional characterization of mixed oxide powders by wet chemical routes is always a challenge to the analysts, because of the refractory nature of constituents. Classical methods, though very accurate and precise, require proficient analysts, rigorous chemical treatments of sample, large chemical /material inventory, and time. Atomic absorption /emission techniques are not suitable for these, due to both the difficulty in dissolution and multi-step dilutions, which in turn will hamper the measurement precision. An instrumental technique, with minimal sample preparation, is ideal to tackle such situations. These analyses can be taken up by energy dispersive X-ray fluorescence (EDXRF) spectrometry. Quantification of major, minor and trace analytes in solids as well as liquids can be carried out using EDXRF [4-6]. Most of the available literature reports on the analysis of solid powder samples proceed via X-ray techniques. Compositional analysis of glass sample has been reported, using XRF to confirm the percentage purity of glass microspheres [7, 8]. The combined analytical techniques like synchrotron µ-XRF, external-PIXE/PIGE (Particle Induced X-ray Emission / Particle Induced Gamma ray emission) and BSEM-EDS (Bench-top Scanning Electron Microscopy equipped with Energy Dispersive Spectroscopy) are also applied to study the different types of glasses [8, 9].

Quantitative XRF analysis proceeds via the calibration standards method [10]. For accurate determinations, it is a pre-requisite that the sample and standard have identical matrices. XRF measurements are influenced by a

Corresponding author. Tel.: *Fax:* +91 22 25505331, Tel: +91 22 25590224; e-mail: psremya@barc.gov.in
https://doi.org/ 10.22034/JCHEMLETT.2023.406725.1123

multitude of factors [11]: (i) the X-ray source flux, energy, spectral distribution, (ii) geometrical set up of measurements, (iii) the sample characteristics such as physical form, size, homogeneity, chemical constitution, the X-ray absorption /emission characteristics of analytes, matrices, fluorescence yields, (iv) detector features: efficiency, dead time, resolution. Among these, the effects due to variation in chemical constitution of the sample are called the inter-element effects [12]. A comprehensive understanding of the inter-element effects is inevitable to ensure accuracy and precision. Various methodologies, adopted by researchers, to address inter-element effects are reviewed in detail by Rousseau [13]. These include the fundamental parameters, basic, modified and hybrid influence coefficient procedures. The fundamental parameter method of XRF has been compared with the k_0-neutron activation analysis and validated for Ni-based alloys by M. Wasim and S. Ahmad [14]. Statistical evaluation of the obtained analytical data has been reported in the literature [15]. Detailed literature survey suggests that there is enough scope for improving the quality and reliability of the results.

The present paper is a report on the systematic examination of the inter-element effects during EDXRF measurements on solid powder samples, and application to mixed oxide samples of aluminium, silicon and yttrium. Subsequently, the results were applied to determine the composition of yttrium aluminium silicate (mixed oxide) samples.

2. Experimental

2.1 Sources of materials, reagents, chemicals, and instrumentation

Spectroscopically pure oxides, viz. Al_2O_3, SiO_2, Y_2O_3 and thin layer chromatography (TLC) grade microcrystalline cellulose powder were obtained from Merck.

All sample, standard and blank pellets were prepared after mixing the required quantities of the respective standard oxides, samples and /or microcrystalline cellulose, in an agate mortar and pestle. For pelletization, the mixtures were transferred to tungsten-coated stainless-steel dies (internal diameter: ~ 10 mm), compressed with the plunger, and applied approximately 5 to 7 tons of pressure using a hydraulic press (KBr press from Techno search, India). The pressed pellets, thus prepared, were carefully removed from the dies, after releasing the pressure.

EDXRF spectrometer (Model: EX-3600M upgraded, Xenemetrix, Israel) was used during all the XRF measurements. The instrument has an in-built Rh X-ray tube with the following specifications [16]: 50 Watt, 50 kV, oil cooled, Be-end window, and front anode. Software tunable solid state power supply applies voltage ranging from 3-50 kV to the X-ray tube, in 1 kV increments (10 to 4000 µA in 1 µA steps). Thermo-electrically cooled silicon drift detector (SDD) does the functions of dispersion and identification of X-rays. The detector has got high counting efficiency (ten lakh counts per second) and energy resolution of 123 eV ± 5 eV at 5.9 keV.

2.2 Preparation of standard pellets

All standard pellets were prepared by mixing individual oxide powders or mixtures of oxide powder with microcrystalline cellulose powder as binder, in an agate mortar and pestle. Then, this mixture is pelletized in clean, dry 10 mm dies, using the hydraulic press. The size of pellets (mass: ~ 200 mg, diameter: ~ 10 mm, thickness: ~ 0.8 mm) was kept same for all standards, samples, and blanks for quantification of analytes in the samples. The pelletization tools, along with the representative pellets of standard and sample, are shown in Fig.1

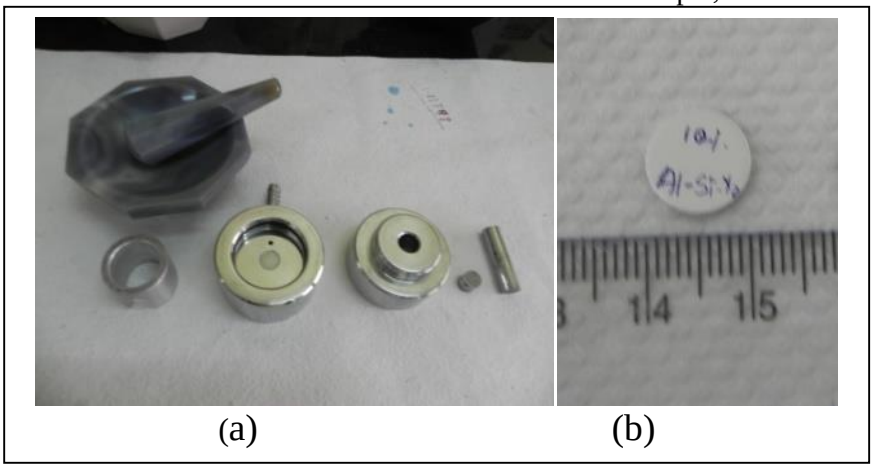

Fig 1. (a) Agate mortar and pestle, tungsten coated stainless steel die having internal diameter of 10 mm, (b) pressed pellets of standard and sample

2.2.1 Preparation of unary oxide pellets

Varying amounts of spectroscopically pure Al_2O_3 (0, 20, 40, 60 mg) were thoroughly mixed with cellulose, pelletized and used as a set of calibration standards for the EDXRF determination of Al. Similarly, individual elemental calibration standard pellets for Si and Y were prepared separately. For this, different amounts of SiO_2 (0, 20, 40, 60, 80 mg), Y_2O_3 (0, 20, 40, 60, 80 mg) were mixed with microcrystalline cellulose powder as the binding agent.

2.2.2 Preparation of binary oxide pellets

Binary oxide pellets were prepared by keeping the amount of one oxide fixed and varying the amount of other oxide. All possible binary combinations of the three oxides, i.e., six sets of standard pellets, were prepared in this manner. Details of these preparations are discussed below.

Two separate sets of binary calibration standard pellets were prepared for Al, in the presence of fixed amounts of SiO_2 and Y_2O_3 as:

i. SiO_2 fixed (~ 80 mg) and Al_2O_3 varied (0 to 60 mg)
ii. Y_2O_3 fixed (~ 80 mg) and Al_2O_3 varied (0 to 60 mg)

Similarly, two sets each of the calibration standards for Si and Y were prepared as:

i. Al_2O_3 fixed (~ 40 mg) and SiO_2 varied (0 to 80 mg)
ii. Y_2O_3 fixed (~ 80 mg) and SiO_2 varied (0 to 80 mg)
iii. Al_2O_3 fixed (~ 40 mg) and Y_2O_3 varied (0 to 80 mg)
iv. SiO_2 fixed (~ 80 mg) and Y_2O_3 varied (0 to 80 mg)

2.2.4 Preparation of ternary oxide pellets

Ternary oxide pellets were prepared by keeping the amounts of two oxides fixed, and varying the third oxide contents in the mixture. Herein, three sets of standard pellets of different compositions were made, as given below:

i. Y_2O_3 fixed (~ 80 mg), SiO_2 fixed (~ 80 mg) and Al_2O_3 varied (0 to 40 mg)
ii. Y_2O_3 fixed (~ 80 mg), Al_2O_3 fixed (~ 40 mg) and SiO_2 varied (0 to 80 mg)
iii. Al_2O_3 fixed (~ 40 mg), SiO_2 fixed (~ 80 mg) and Y_2O_3 varied (0 to 80 mg)
iv.

2.3 EDXRF analysis

All pellets were analyzed under optimized acquisition parameters. The KL_3 (K_α) X-rays were monitored for Al and Si. In the case of Y, both the KL_3 and L_3M_5 ($L_{\alpha 1}$) X-ray intensities were recorded. Based on the dead time of detector and counting statistics (criterion for good counting statistics is to obtain a minimum of 10,000 net counts for each characteristic X-ray peak), two separate sets of acquisition parameters were used during the present measurements. Optimized parameters for monitoring the Al-KL_3, Si-KL_3 and Y-L_3M_5 X-rays were: X-ray tube voltage: 5 kV, current: 2000 µA, energy range: 10 keV, acquisition time: 200 s, medium: vacuum and with no filter. While using Y-KL_3 X-rays, the optimized measurement parameters were: voltage: 35 kV, current: 100 µA, range: 40 keV, acquisition time: 50 s, medium: air and with Rh filter. Characteristic X-rays used during the present work, are given in Table 1 along with their energies [17], absorption edges [18] and their relevant regions of interest (ROI) in the X-ray spectra.

Table 1. Relevant factors for optimizing the EDXRF measurements

Element	X-ray notation	Energy (keV)	Absorption edge (keV)	Region of interest (keV)
Al	KL_3	1.487	1.559	1.320-1.600
Si	KL_3	1.740	1.838	1.610-1.810
Y	L_3M_5	1.922	2.369	1.830-2.100
Y	KL_3	14.958	17.037	14.480-15.240

2.3.1 Calibration of the spectrometer using set of standard pellets

Calibrations for Al, Si and Y were performed using the above prepared 12 sets of standards, keeping concentrations of other element /elements constant. Calibration curves for Al were constructed, using pure Al_2O_3, in the presence of SiO_2, Y_2O_3 and (SiO_2 + Y_2O_3). Similarly, calibration curves for Si were constructed using pure SiO_2, in the presence of Al_2O_3, Y_2O_3 and (Y_2O_3 + Al_2O_3). Calibration curve for Y was made, using pure Y_2O_3, in the presence of Al_2O_3, SiO_2 and (Al_2O_3 +SiO_2), under the above optimized acquisition parameters.

2.3.2 Inter-element effects on the EDXRF calibration of Al, Si and Y

Calibration curves for pure Al (0, 20, 40, 60 mg as oxide) were compared with those obtained in the presence of Si (~ 80 mg as oxide) and Y (~ 80 mg as oxide) as the matrices. Similarly, calibration curves for pure Si (0, 20, 40, 60, 80 mg as oxide) were compared with those obtained

in the presence of Al (~ 40 mg as oxide) and Y (~ 80 mg as oxide). Similar comparisons were done for Y also. Slope and intercept were obtained from each calibration curve and compared with those of the pure elements. These results were used as tools to establish the inter-element effects during EDXRF analysis.

2.3.3 Sample analysis

Yttrium aluminium silicate glass and yttrium aluminium silicate microsphere samples were analyzed for Al, Si and Y. Series of standards and blank were prepared by varying analyte and fixing other two elements which is considered as matrix as mentioned above in section 2.2.3. The samples were finely ground, homogenized, accurately weighed (~200 mg) and pelletized using the KBr press mentioned in section 2.2. All the samples, standard and blank pellets were analyzed by EDXRF using optimized acquisition parameters, as mentioned in section 2.3. The net counts of all the analytes were noted down. Separate linear calibration curves were constructed by plotting the net counts vs the respective analyte amounts in the standard pellets. From the net counts of analytes in the sample pellets, Al, Si and Y were quantified, using the 'respective linear calibration functions'. These 'respective linear calibrations' are the one's obtained for matrix matching, ternary oxide pellet standards for each analyte.

3. Results and discussion

Calibration standard pellets of unary (pure single elemental standard pellets), binary, and ternary oxide mixtures were utilized for studying the inter-element effects on the EDXRF calibration of Al, Si and Y. Further, the effects were correlated with the theoretical factors and specific measurement conditions.

XRF measurements are heavily affected by the sample matrix characteristics, in addition to those of the analytes [19, 20]. If we compare pure, separate uni-element systems, with multi-element systems, the detected fluorescence signals for the latter are found to get drastically modified due to various interactions with the sample matrix. Hence, it is imperative that while proceeding from pure, single analyte systems to real sample analyses, we have to consider the effects of other elements [21-24]. The effect is more pronounced in EDXRF, when a low atomic number analyte is to be determined in a high atomic number matrix. Therefore, knowledge of the inter-element effects is inevitable for the appropriate utilization of the available tools.

3.1 Calibration of the spectrometer using set of standard pellets and the inter-element effects

Figure 2 shows the EDXRF calibration curves for pure Al-KL_3 X-rays, effects of fixed amounts of Si and Y separately (the binary oxide mixtures) and the combined effects of Si and Y (ternary oxide mixtures), on the calibration curve for Al. Similarly, Figs. 3, 4 and 5 show the inter-element effects on the calibrations for Si-KL_3, Y-L_3M_5 and Y-KL_3 respectively. Table 2 summarizes the figures of merit, such as the sensitivity, intercept and the R^2, of these calibration curves.

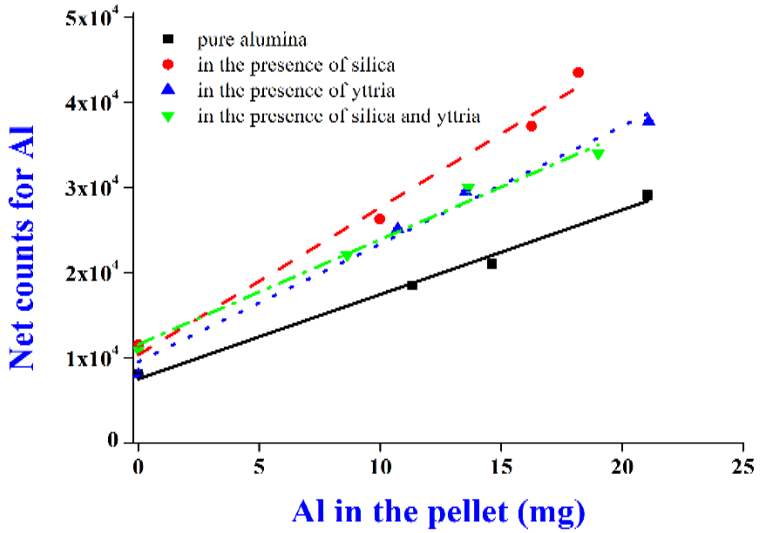

Fig 2. Calibration curves for Al-KL_3 X-rays and the effects of presence of SiO_2 and Y_2O_3

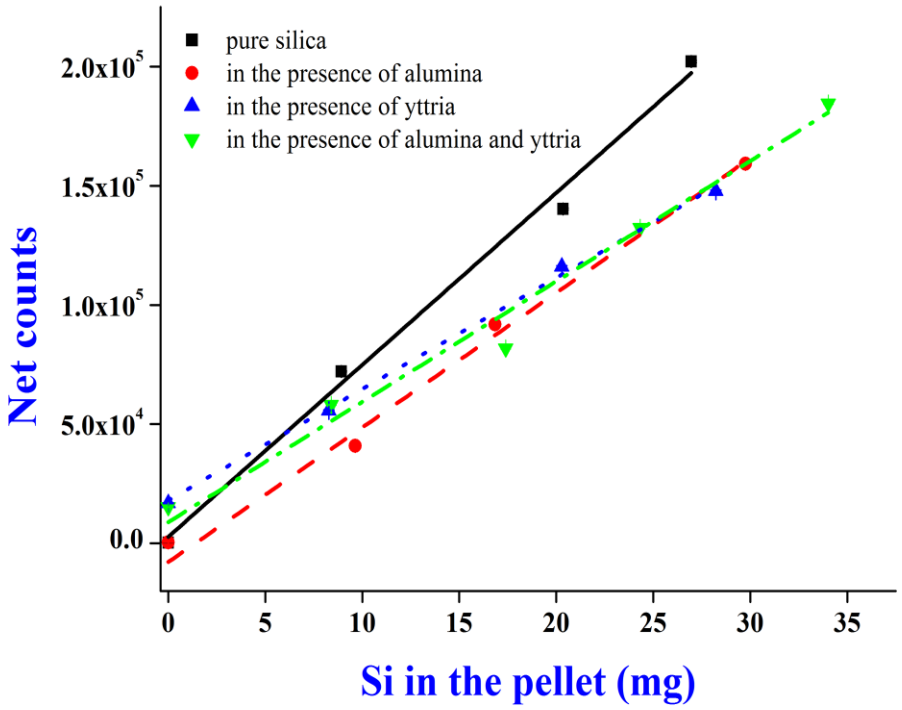

Fig 3. Calibration curves for Si-KL_3 X-rays and the effects of presence of Al_2O_3 and Y_2O_3

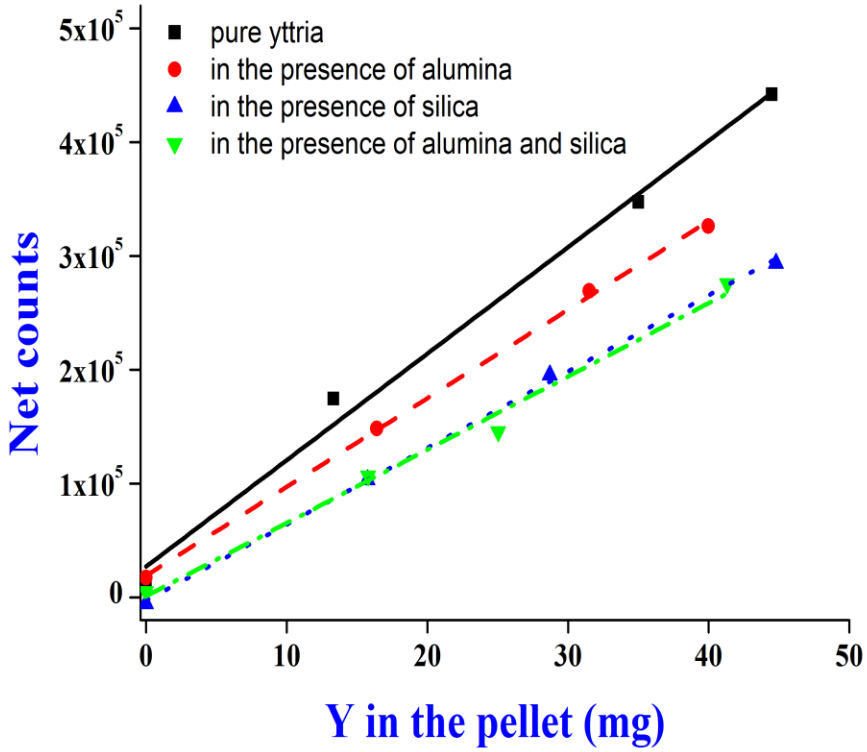

Fig 4. Calibration curves for Y-L_3M_5 X-rays and the effects of presence of Al_2O_3 and SiO_2

Table 2. Features of EDXRF calibration curves and the inter-element effects

Sl. No.	Description	Oxide matrix in cellulose	Analyte	Slope (counts per mg of analyte)	Intercept	R^2
1	Pure Al_2O_3	--	Al	994	7506	0.985
2	SiO_2 Fixed-Al_2O_3	SiO_2	Al	1731	10357	0.976
3	Y_2O_3 Fixed-Al_2O_3	Y_2O_3	Al	1383	9547	0.980
4	Y_2O_3 fixed-SiO_2 fixed-Al_2O_3	Y_2O_3, SiO_2	Al	1232	11571	0.976
5	Pure SiO_2	--	Si	7214	2762	0.977
6	Al_2O_3 Fixed-SiO_2	Al_2O_3	Si	5648	-7824	0.990
7	Y_2O_3 Fixed-SiO_2	Y_2O_3	Si	4665	18118	0.996
8	Y_2O_3 fixed-Al_2O_3 fixed-SiO_2	Y_2O_3, Al_2O_3	Si	5049	8922	0.974
9	Pure Y_2O_3	--	Y	9355	27083	0.989
10	Al_2O_3 Fixed-Y_2O_3	Al_2O_3	Y	7785	19365	0.999
11	SiO_2 Fixed-Y_2O_3	SiO_2	Y	6708	-2828	0.998
12	Al_2O_3 fixed-SiO_2 fixed-Y_2O_3	Al_2O_3, SiO_2	Y	6439	935	0.985

From Figs. 2, 3, 4 and Table 2, it is clear that the sensitivities (also called slope of the calibration plot) of the spectrometer for pure Al, Si and Y are 994 counts mg^{-1}, 7214 counts mg^{-1} and 9355 counts mg^{-1} respectively. The sensitivity values were found to increase gradually from Al to Y, in agreement with the atomic numbers, mass attenuation coefficients of the analytes for source X-rays and the respective fluorescence yields [4, 11]. The energies of characteristic X-rays also are in the same ascending order, when we move from Al to Si to Y, as can be seen in Table 1. The intercepts for pure Al, Si and Y were 7506, 2762 and 27083 respectively. The intercepts could be arising due to the backgrounds at the respective regions, from the X-ray tube source [25].

A comparison of the calibration function of Al with those obtained in the presence of the other two oxides can be made, with the help of Table 2 and Fig.3. Presence of fixed amounts of SiO_2 and Y_2O_3 led to increase in the slope for Al from 994 to 1731, 1383 counts mg^{-1} respectively. The slope of the calibration curve increased to 1232 counts mg^{-1}, during the analysis of ternary oxides mixture [varying amounts of Al, in the presence of fixed amounts of (SiO_2 + Y_2O_3)]. The increasing effect of slope could be attributed to the enhancement of analytical signal (of Al-KL_3) from Si-KL_3 and Y-L_3M_5 X-rays (1.740 and 1.992 keV) which lie just above the absorption edge of Al (1.559 keV). This enhancement is more pronounced in the presence of Si than Y, due to the higher proximity of the matrix characteristic X-rays to the analyte absorption edge. Even though the matrix X-rays enhance the generation of characteristic X-rays of Al, these higher Z-matrices pose attenuation, which resulted in the observed slope, during ternary oxide analysis.

Addition of fixed amounts of SiO_2, Y_2O_3 and (SiO_2 + Y_2O_3) resulted in the increase in intercept of the curve of Al from 7506 (pure Al_2O_3) to 10357, 9547 and 11571 respectively. The increase in intercept could be due to the Compton background [25], arising from Si and Y X-rays.

Now, consider the calibration curve for Si in unary, binary and ternary oxide mixture pellets (Fig. 4). The slope decreased from 7214 (in pure SiO_2) to 5648 and 4665 counts $mg^{-1}$of Si, upon addition of fixed amounts of Al_2O_3 and Y_2O_3 respectively. In the ternary oxide mixture also, slope of the calibration curve of Si reduced to 5049 counts mg^{-1}. Al absorbs the Si-KL_3 X-rays and hence the observed reduction in slope of SiO_2. The Y-L_3M_5 X-rays may act as additional excitation source, since their energy (1.992 keV) is just above the absorption edge of Si (1.838 keV). However, at the same time, the high atomic number Y matrix may cause attenuation of the Si characteristic X-rays. Among these two, the attenuation by Y exceeds the enhancement effect, on Si X-rays. Hence, the final outcome of these opposing effects is the observed lowering of slope for Si. Similar explanation holds in the case of ternary oxide too.

Intercept of the curve decreased drastically from 2762 (in pure SiO_2) to -7824 (with fixed Al_2O_3). This could be due to reduced background at the region of interest for Si, as a result of absorption by Al. Addition of fixed Y_2O_3, led to a rise in intercept upto 18118 counts. In the ternary oxide mixture also, intercept of the calibration for Si went up to 8922 counts. These results show the predominance of Y over Al in elevating the background at the region of Si X-rays. Another contribution to the high background from Y could be visualized from the overlap of Si and Y characteristic X-rays in the acquired spectra. The

instrumental ROI did not take care of this spectral interference. In order to alleviate the background effects, the ROI's for Si and Y were manually marked during the entire measurements, as shown in Table 1.

In the case of pure Y_2O_3, the slope of the calibration curve was 9355 counts mg^{-1} of Y (Fig. 5). The slope decreased upon addition of both Al and Si to 7785 and 6708 counts mg^{-1} of Y, in the respective binary oxides. In the ternary oxides, a cumulative decrease in slope was observed, i.e., to 6439 counts mg^{-1}. The decrease in slope may be attributed to the absorption [25] of Y X-rays by Al and Si. Intercept of the curve decreased from 27083 (in pure Y_2O_3) to 19365 and -2828 counts upon addition of Al and Si respectively. In the case of ternary oxide pellets, the intercept was 935 counts. The decrease in intercept, in other words: the lower background at the region of interest for Y, is the result of reduced scattering in the presence of lighter matrices [13] Al_2O_3 and SiO_2.

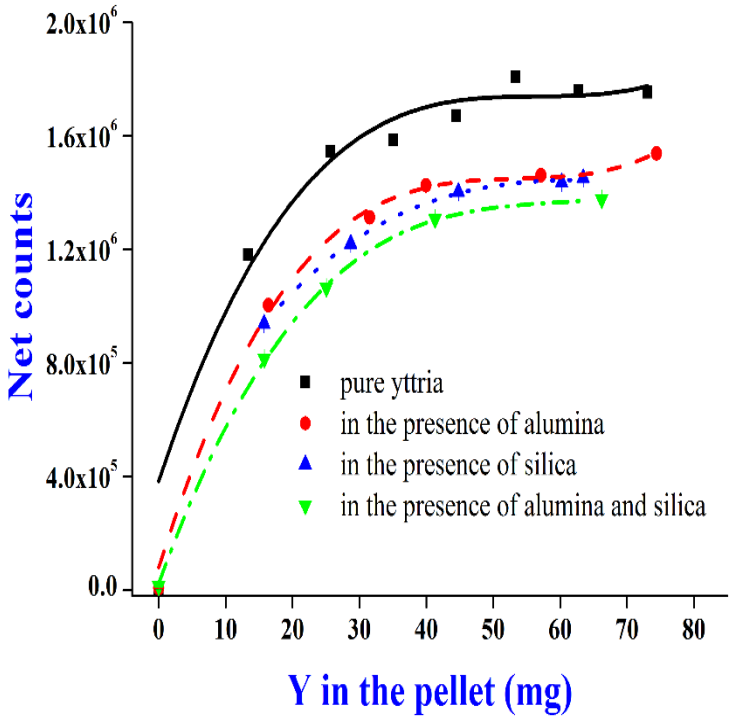

Fig 5. Calibration curves for Y-KL_3 X-rays and the effects of presence of Al_2O_3 and SiO_2

As shown in Fig. 5, the net counts vs amount of Y curve reached saturation for the KL_3 X-ray lines, in the studied range. Here, the net counts were one order of magnitude higher than those for Y-L_3M_5 X-rays, on account of the higher fluorescence yield ($\omega_k = 0.7093$, $\omega_L = 0.0289$) [26], lower attenuation, scattering in matrix as well as sample environment [4]. The curve was best fitted in a 3rd order polynomial function between the net counts and amount of Y. Even in this curve, the inter-element effects were visible in each coefficient of the polynomial. The overall trends were similar to those observed in the case of Y-L_3M_5 X-ray lines (Fig. 4). Hence, similar explanations holds good for Fig. 5 too.

3.3 Application to sample analysis

Yttrium aluminium silicate glass powder and microsphere samples were analysed for Al, Si and Y content. Percentage of Al, Si and Y were determined by EDXRF technique. The percentage of Si was verified by gravimetry. Si suffers from severe inter-element effects, due to the proximate presence of X-rays at both lower (Al-KL_3) and higher (Y-L_3M_5) energy sides. A typical EDXRF spectrum, acquired under the optimized parameters of 5 kV, 2000 μA, 10 keV, 100 s, vacuum, without source filter, for one of the samples is shown Fig.6.

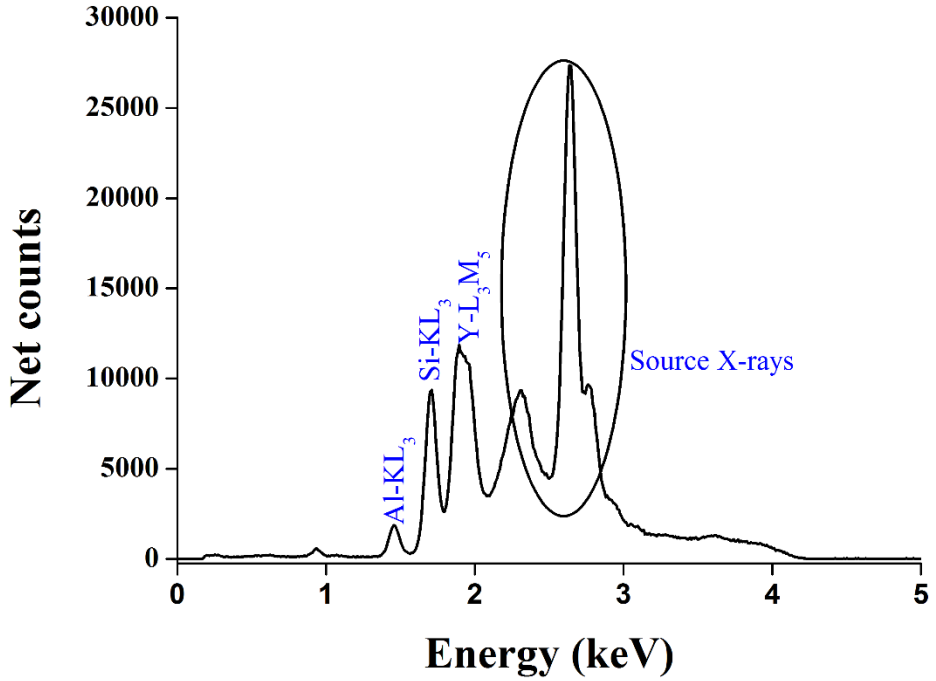

Fig 6. Typical EDXRF spectrum of yttrium aluminium silicate sample

The characteristic X-rays, namely the KL_3 lines of Al, Si and L_3M_5 line of Y, are visible in this spectrum, along with the source X-ray peaks. Table 3 summarizes the results of analysis of 4 replicates on each sample, via the matrix-matching calibration standards containing ternary oxide mixtures.

Table 3. Results of EDXRF analysis of yttrium aluminium silicate samples

Sample ID	Al_2O_3 (%)	SiO_2 (%)	Y_2O_3 (%)
YAS glass powder	18.0 ± 1.6	39.3 ± 0.25	43.2 ± 3.0
YAS glass microspheres	19.4 ± 1.3	40.4 ± 0.24	40.1 ± 2.6

Note: Number of replicates, n= 4 for each sample

The inter-element effects can be visualized from Table 4.

Table 4. Inter-element effects on the results obtained for samples, using various matrices for calibration

Analyte	% relative error with respect to ternary system, while using:		
Al	pure single element calibration	binary with SiO_2	binary with Y_2O_3
	151	-7.1	34.5
	162	-5.1	38.6
Si	pure single element calibration	binary with Al_2O_3	binary with Y_2O_3
	-22.4	15.9	-9.4
	-21.4	19.2	-11.6
Y	pure single element calibration	binary with Al_2O_3	binary with SiO_2
	-45.4	-29.3	-1.2
	-45.3	-29.3	-1.2

Herein, the percentage relative errors of the values obtained for various systems are shown with respect to the respective matrix-matching ternary calibration systems. From a comparison of the unary-ternary calibrations, it is visible that the highest loss in accuracy is obtained for the pure single element calibration system, in comparison with its ternary analogue. Among the three, Si has got least variation, as a result of the cancellation of opposing effects

due to the presence of low Z (Al) as well as high Z (Y) matrix elements. Now, compare between binaries and ternaries. In the case of Al, the binary with SiO_2 showed the least deviation. This signifies that Si is the major contributor to matrix effects for Al. In the case of Si, the binary with Y_2O_3 showed the least deviation with respect to the ternary system. Thus, Y is the dominant in influencing the Si X-rays. In similar lines, it can be concluded that Si dominates over Al, in modifying the Y-L_3M_5 X-ray intensities. Same explanation holds for the Y-KL_3 lines also, where the (net counts vs amount Y) curve shows a 3rd order polynomial relationship, owing to the saturation of counts.

4. Conclusions

Inter-element effects during the determination of Al, Si and Y in yttrium aluminium silicate samples, using EDXRF, were investigated. The effects of other elements on the calibration curves of each analyte were evaluated, by systematic investigation of standard pellets of unary, binary and ternary oxide mixtures. The increase in sensitivity while moving from Al to Si to Y, was expected as per their X-ray respective X-ray absorption/emission characteristics: atomic numbers, energies of the characteristic X-rays, absorption edge, reported mass absorption coefficients, fluorescence yields and attenuation. Addition of other oxides affected the instrumental sensitivities, which was the accumulated effect of various factors such as the characteristic X-ray energies, absorption of source X-rays due to the matrix, enhanced interactions near the absorption edge and attenuation of analyte X-rays in the matrix. The variations in intercepts could be because of the scattering of source /characteristic X-rays in the sample, overlap of peaks and absorption /enhancement by the matrices. Among all the matrix-analyte combinations studied, the largest inter-element effects were recorded for the combinations: Si-Al, Y-Si, and Si-Y. Thus, it is lucid from the present studies, that the Si matrix plays a major role in modifying the analytical signals of both Al and Y, during EDXRF analyses.The properly preserved calibration standards can be re-used as many times as possible, for the fast and precise analysis of similar samples. The present results can be extended for determination of the major constituents in other binary and ternary alloys and oxides.

Acknowledgements

The authors acknowledge the guidance and support by Dr. C.N. Patra, Head, Analytical Chemistry Division, BARC, Mumbai, India.

References

[1] S. Kumar, R.S. Nair, A. Dixit, M.G. Sawant, P. Mollick, M. Goswami and A.K. Arya, Development of yttrium-alumino-silicate glass microspheres for HCC radiotherapy application. BARC newsletter September-October (2022) 48-53.

[2] M.J. Hyatt and D.E. Day, Glass properties in the yttria-alumina-silica system. *J. Am. Ceram. Soc.*, 70 / l0 (1987) C-283-C-287. doi.org/10.1111/j.1151-2916.1987.tb04901.x

[3] R. Salem, R.J. Lewandowski, B. Atassi, S.C Gordon, V.L Gates, O. Barakat, Z. Sergie, C.Y.O Wong and K.G Thurston, Treatment of unresectable hepatocellular carcinoma with use of ^{90}Y microspheres (TheraSphere): Safety, tumor response and survival. *J. Vasc. Interv. Radiol.*, 16 (2005) 1627-1639. doi.org/10.1097/01.RVI.0000184594.01661.81

[4] E.P. Bertin, Principles and practice of X-ray spectrometric analysis, 2nd Edition (1984) Plenum Press, New york-London. pp 89-112.

[5] P.J. Potts, X-ray fluorescence and emission/X-ray fluorescence theory, Encyclopaedia of analytical science, 2nd edition (2005) pp 408-418. doi.org/10.1016/B0-12-369397-7/00673-7

[6] J.F.F. Masulli, P. Kump and E. González, Selected trace and minor elements in sandstones from Paraguay. *Radiochim. Acta*., 97 / 7 (2010) 441-446. doi.org/10.1524/ract.2010.1734

[7] Glass microspheres (Patent) WO 86/03124, US (1986) PCT/US85/02207. The curators of the University of Missouri, 227, University Hall, Columbia, MO 65211.

[8] M.R. Ghahramani, A.A. Garibov and T.N. Agayev, Production of yttrium aluminum silicate microspheres by gelation of an aqueous solution containing yttrium and aluminum ions in silicone oil. Int. J. Radiat. Res., 12 / 2 (2014) 179-187.

[9] N. Schiavon, A. Candeias, T. Ferreira, M.C. Lopes, A. Carneiro, T. Calligaro and J. Mirao, A combined multi-analytical approach for the study of roman glass from south-west Iberia: Synchrotron μ-XRF, external-PIXE/PIGE and BSEM-EDS. *Archaeometry*, 54 / 6 (2012) 974-996. doi.org/10.1111/j.1475-4754.2012.00662.x

[10] A. Markowicz, An overview of quantification methods in energy dispersive X-ray fluorescence analysis. *Pramana-J. Phys*., 76 (2011) 321-329. doi: 10.1007/s12043-011-0045-z

[11] R. Sitko and B. Zawisza, Quantification in X-ray fluorescence spectrometry. Available online at https://www.intechopen.com/download/pdf/27342, Intechopen.com (2012) Poland, pp 137-138.

[12] R.M. Rousseau, Concept of the influence coefficient. *The Rigaku Journal*., 18 / 1 (2001) 8-21.

[13] R.M. Rousseau, Corrections for matrix effects in X-ray fluorescence analysis - A tutorial. *Spectrochimica Acta Part B*., 61 (2006) 759 - 777. doi:10.1016/j.sab.2006.06.014

[14] M. Wasim and S. Ahmad, Comparison of two semi-absolute methods: k_0-instrumental neutron activation analysis and

fundamental parameter method X-ray fluorescence spectrometry for Ni-based alloys. *Radiochim. Acta*, 103 / 7 (2015) 533-540. doi.org/10.1515/ract-2014-2364

[15] D.A. Skoog, F.J. Holler and T.A. Nieman, Principles of Instrumental Analysis, 5th Edition (2006) Thomson business information India private limited, New Delhi. pp15-18

[16] Operation manual nEXt series, EX-3600/6600 XRF spectrometers, P/N 069-000002-00, Revision 2.0 (2000) Chapter 3, Jordan Valley AR, Ltd, POB 103, Migdal Haemek, 23100, Israel

[17] https://physics.nist.gov/PhysRefData/XrayTrans/Html/search.html; Accessed on 12th May 2023

[18] https://physics.nist.gov/PhysRefData/XrayMassCoef/tab3.html; Accessed on 12th May 2023

[19] R.T. Mainardi, J.E. Fernández and M. Nores, Influence of inter-element effects on X-ray fluorescence calibration curve coefficients for binary mixtures. *X-ray Spectrom*., 11 /2 (1982) 70-78. doi.org/10.1002/xrs.1300110209

[20] Y. Wang, X. Zhao and B.R. Kowalski, X-ray fluorescence calibration with partial least squares. *Appl. Spectroscopy*, 44 /6 (1990) 998-1002. doi.org/10.1366/0003702904086867

[21] R. Tertian, Quantitative chemical analysis with X-ray fluorescence spectrometry-an accurate and general mathematical correction method for the inter-element effects. *Spectrochim. Acta B: Atom. Spectroscopy*, 24 / 8 (1969) 447-471. doi.org/10.1016/0584-8547(69)80046-7

[22] J. Lucas-Tooth and C. Pyne, The accurate determination of major constituents by X-ray fluorescent analysis in the presence of large inter-element effects. *Advances in X-ray Analysis*, 7 (Twelfth annual conference on applications of X-ray analysis, August 7-9 (1963) 523-541. doi.org/10.1154/S0376030800002780

[23] S.D. Rasberry and K.F.J. Heinrich, Calibration for inter-element effects in X-ray fluorescence analysis. *Anal. Chem.*, 46 / 1 (1974) 81-89. doi.org/10.1021/ac60337a027

[24] C. Shenberg and S. Amiel, Critical evaluation of correction methods for inter-element effects in X-ray fluorescence analysis applied to binary mixtures. *Anal. Chem.*, 46 /11 (1974) 1512-1516. doi.org/10.1021/ac60347a021

[25] P.S. Remya Devi, T.A. Chavan, S.S. Shitole, P.M. Gawade and K.K. Swain, Insights into the inter-element effects in the EDXRF determination of zirconium in binary aqueous solutions via the calibration method. *Anal. Chem. Lett.*, 11/1 (2021) 83-101. doi.org/10.1080/22297928.2021.1886986

[26] K. Meddouh, S. Daoudi, A. Kahoul, J.M. Sampaio, J.P. Marques, F. Parente, N. Kup Aylikci, V. Aylikci, Y. Kasri and A. Hamidani, Average K-, L-, and M-shell fluorescence yields: A new semi-empirical formulae. *Radiat. Phys. Chem*., 202 (2023) 11048-110496. doi.org/10.1016/j.radphyschem.2022.110481